An Essential Role for Ectodomain Shedding in Mammalian Development

Jacques J. Peschon,* Jennifer L. Slack, Pranitha Reddy, Kim L. Stocking, Susan W. Sunnarborg, David C. Lee, William E. Russell, Beverly J. Castner, Richard S. Johnson, Jeffrey N. Fitzner, Rogely W. Boyce, Nicole Nelson, Carl J. Kozlosky, Martin F. Wolfson, Charles T. Rauch, Douglas Pat Cerretti, Raymond J. Paxton, Carl J. March, Roy A. Black

The ectodomains of numerous proteins are released from cells by proteolysis to yield soluble intercellular regulators. The responsible protease, tumor necrosis factor-α converting enzyme (TACE), has been identified only in the case when tumor necrosis factor-α (TNFα) is released. Analyses of cells lacking this metalloproteinase-disintegrin revealed an expanded role for TACE in the processing of other cell surface proteins, including a TNF receptor, the L-selectin adhesion molecule, and transforming growth factor-α (TGFα). The phenotype of mice lacking TACE suggests an essential role for soluble TGFα in normal development and emphasizes the importance of protein ectodomain shedding in vivo.

Members of the ADAM (A Disintegrin And Metalloproteinase) family of metalloproteinases are membrane proteins that contain both metalloproteinase and disintegrin domains (*1*). The first member to be characterized was identified through its ability to mediate cell-cell interactions (*2*). Although a number of ADAMs have been identified in both mammals and invertebrates, and many of these are predicted to encode active metalloproteinase domains, TACE (ADAM17) is the only mammalian metalloproteinase-disintegrin with known catalytic function, namely, processing of TNF (*3, 4*). In *Drosophila*, proteolytic processing of the extracellular domain of Notch depends on the ADAM kuzbanian (*5*), and the related ADAM in *Caenorhabditis elegans*, SUP-17, may have a similar role (*6*). Thus, ADAMs participate in the proteolytic processing of two distinct membrane-anchored proteins.

Many functionally diverse proteins, including cytokines, growth factors, and their receptors, are initially synthesized as membrane-anchored moieties that are subsequently released from the cell by proteolysis (*7*); however, the proteinases mediating specific cleavage of these proteins remain undefined except in the case of TNF. Despite the diversity in structure, cell type distribution, membrane topology, and cleavage site sequence of these shed proteins, two lines of evidence suggest a common mechanism for ectodomain processing. First, the majority of shedding events are inhibited by metalloproteinase inhibitors (*7*). Second, mutant cell lines defective in the release of multiple unrelated ectodomains have been isolated (*8*). The activities of TACE and kuzbanian indicate that a common mechanism for ectodomain processing may be ADAM-directed proteolysis.

The physiological significance of ectodomain shedding remains in most cases undefined. Various cytokines and growth factors are biologically active when retained on the cell surface. Thus, surface localization may serve to restrict activity to specific microenvironments, whereas release may lead to distal effects. Membrane-anchored ligands are also proposed to deliver qualitatively different signals than those provided by the respective soluble ligands (*9*). Shed receptors may further serve to regulate the biological activity of these ligands by acting as agonists or antagonists, and receptor shedding may additionally render cells less responsive to their cognate ligands (*10*). We present evidence for a broad role of a single metalloproteinase-disintegrin, TACE, in the shedding of a diverse group of membrane-anchored proteins. Perinatal and postnatal defects in mice lacking this enzyme were associated with numerous epithelial anomalies and revealed an essential role for a metalloproteinase-disintegrin during mammalian development.

Essential role for TACE during mouse development. Cultured cells homozygous for a targeted mutation in TACE ($tace^{\Delta Zn/\Delta Zn}$), which deletes the Zn^{2+} binding domain and thus inactivates metalloproteinase activity, fail to efficiently release TNF (*3*). To examine the consequences of this mutation in vivo, we generated $tace^{\Delta Zn/\Delta Zn}$ mice. Genotype analyses of progeny derived from $tace^{\Delta Zn/+}$ intercrosses revealed an underrepresentation of $tace^{\Delta Zn/\Delta Zn}$ mice at 2 to 3 weeks of age (Table 1). Lethality could not be attributed to a loss of soluble TNF function because mice lacking TNF or its receptors (TNFRs) are overtly normal (*11*). The $tace^{\Delta Zn}$ mutation was also lethal in mice lacking both TNFRs ($p55^{-/-}$ $p75^{-/-}$), indicating that lethality was not due to inappropriate triggering of TNFRs by uncleaved TNF (Table 1). Thus, lethality associated with the $tace^{\Delta Zn}$ mutation was TNF independent and suggested an expanded role for TACE in the processing of other membrane-anchored proteins, one or more of which is essential for development.

The majority of $tace^{\Delta Zn/\Delta Zn}$ mice died between embryonic day 17.5 (e17.5) and the first day after birth (Table 1) (*12*). All newborn $tace^{\Delta Zn/\Delta Zn}$ mice could be identified by the presence of stunted vibrissae and open eyelids (*12*). Eyelids normally fuse at about e16.5 and do not open until about postnatal day 14 (P14) (*13*). In contrast, all $tace^{\Delta Zn/\Delta Zn}$ fetuses on e17.5 had open eyelids resulting from a failure of eyelid fusion, lacked a conjunctival sac, and had attenuated corneas

J. J. Peschon, J. L. Slack, P. Reddy, K. L. Stocking, B. J. Castner, R. S. Johnson, J. N. Fitzner, N. Nelson, C. J. Kozlosky, M. F. Wolfson, C. T. Rauch, D. P. Cerretti, R. J. Paxton, C. J. March, and R. A. Black are with Immunex Corporation, 51 University Street, Seattle, WA 98101, USA. S. W. Sunnarborg and D. C. Lee are in the Department of Biochemistry and Biophysics, University of North Carolina, Chapel Hill, NC 27599–7260, USA. W. E. Russell is in the Departments of Pediatrics and Cell Biology, Vanderbilt University, Nashville, TN 37232, USA. R. W. Boyce is with Pathology Associates International, Frederick, MD 21701, USA.

*To whom correspondence should be addressed. E-mail: peschon@immunex.com

Table 1. Genotyping of progeny derived from $tace^{\Delta Zn/+}$ intercrosses. The numbers of viable progeny corresponding to each genotype are listed. Additional nonviable $tace^{\Delta Zn/\Delta Zn}$ fetuses are indicated in parentheses. Most $tace^{\Delta Zn/\Delta Zn}$ mice found alive at birth died within several hours (*12*). The six surviving $tace^{\Delta Zn/\Delta Zn}$ mice were either killed or found dead between P14 and P21. The genotyping assay could not distinguish between +/+ and ΔZn/+ on a $p55^{-/-}$ $p75^{-/-}$ background. Animal care was in accord with Immunex institutional guidelines. e, embryonic; P, postnatal; nd, not determined.

Background	Age	Total	+/+	ΔZn/+	ΔZn/ΔZn
C57BL/6 × 129	e13.5–16.5	100	25	52	20 (3)
	e17.5–18.5	103	23	59	17 (4)
	P14–21	464	163	295	6
$p55^{-/-}p75^{-/-}$	P14–21	51	nd	nd	0

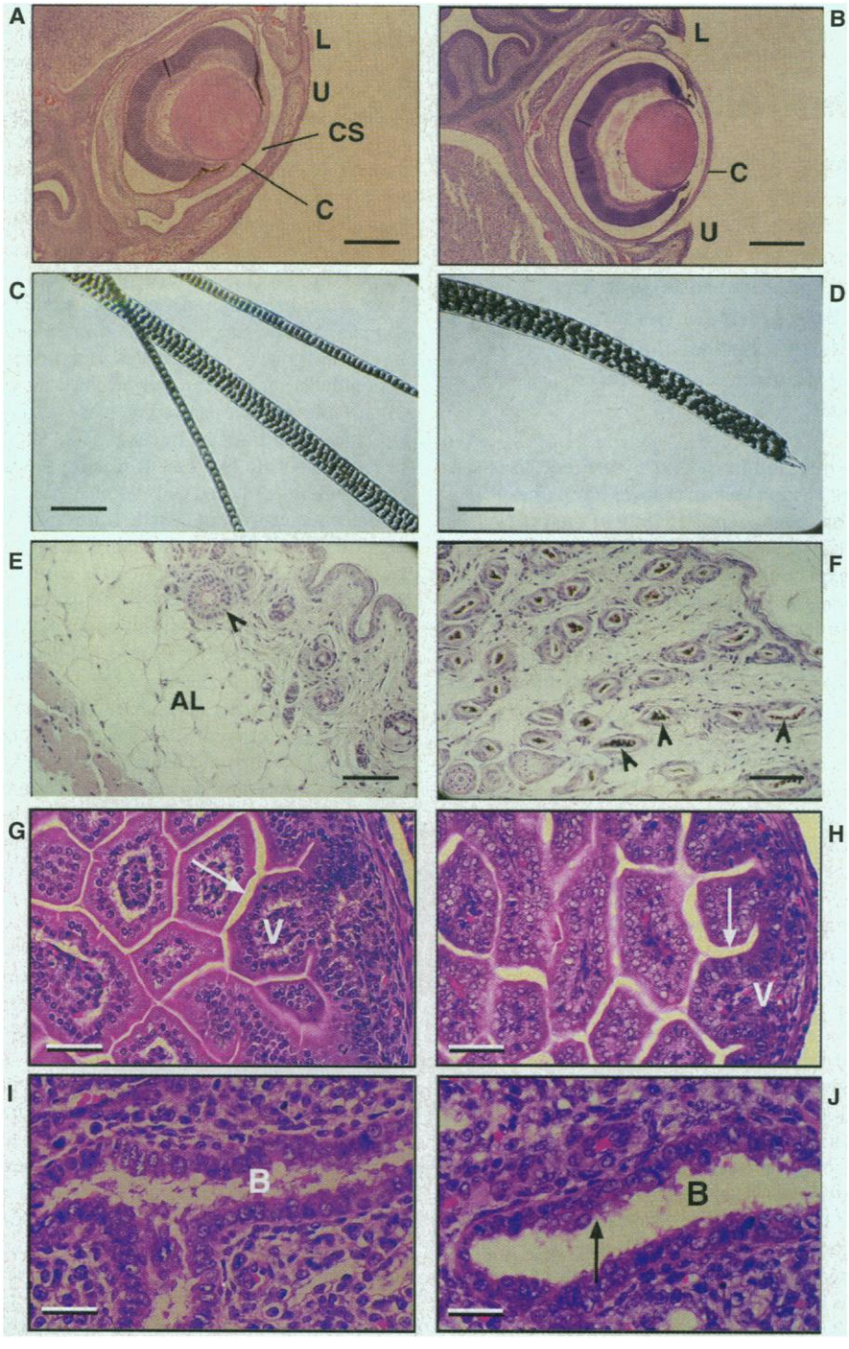

Fig. 1. Eye, hair, and skin defects associated with *tace*$^{\Delta Zn}$ mutation revealed in hematoxylin- and eosin-stained tissues. Transverse sections of e17.5 wild-type (**A**) and *tace*$^{\Delta Zn/\Delta Zn}$ (**B**) eyes revealed a failure of fusion between upper (U) and lower (L) eyelids and an attenuated cornea (C) in the mutant. The conjunctival sac (CS) was absent in the mutant (bar = 267 μm). Surviving P19–21 *tace*$^{\Delta Zn/\Delta Zn}$ (**D** and **F**) mice and control littermates (**C** and **E**) revealed abnormal, irregular pigment deposition within pelage hairs derived from the mid-dorsum (D) and altered skin morphology evident on stained sections (F). Hair follicles (arrowhead) were absent from the adipose layer (AL) of control skin (E) but were randomly distributed within this layer in the mutant (F). *tace*$^{\Delta Zn/\Delta Zn}$ hair follicles were densely distributed, had irregular shapes, and contained hairs with disorganized pigment deposits (arrowheads) (bar, 20 μm). Sections of the proximal small intestine from wild-type (**G**) and *tace*$^{\Delta Zn/\Delta Zn}$ (**H**) e17.5 fetuses revealed variably blunted villi (V) and a hypercellular, pseudostratified mucosal epithelium (arrow) displaying less cell polarity (bar, 54 μm). Sections of the lung of wild-type (**I**) and *tace*$^{\Delta Zn/\Delta Zn}$ (**J**) e17.5 fetuses revealed impaired differentiation of the bronchiolar epithelium. Bronchioles (B) were lined by epithelium that appeared disorganized with variable hypercellularity, segmental stratification (arrow), and increased nuclear to cytoplasmic ratio (bar, 27 μm). Tissue preparation described in (*31*).

(Fig. 1, A and B). Those few *tace*$^{\Delta Zn/\Delta Zn}$ mice that survived for several weeks had body weights 20 to 40% less than those of littermates. Additionally, they displayed various degrees of eye degeneration with apparent corneal inflammation, perturbed hair coats, curly vibrissae, and dense, irregular pigmentation patterns within pelage hairs (Fig. 1, C and D) (*12*). Histological sections of *tace*$^{\Delta Zn/\Delta Zn}$ skin from the mid-dorsum revealed a disorganized distribution and structure of hair follicles, which were irregularly positioned and oriented, extended into the adipose layer, and contained hairs with irregular pigment deposition (Fig. 1, E and F).

Histological examination of *tace*$^{\Delta Zn/\Delta Zn}$ fetuses on e17.5 revealed multiple additional defects, primarily in epithelial cell maturation and organization. Epithelial dysgenesis characterized by delayed or impaired maturation was observed in multiple organs, including the intestine, lung, nonglandular stomach, thyroid, parathyroid, and salivary gland (Fig. 1, G through H) (*14*). Additionally, *tace*$^{\Delta Zn/\Delta Zn}$ placentas displayed a mild attenuation of the spongiotrophoblast layer associated with a disorganized and discontinuous plate of giant trophoblast cells (*14*). Defects in both the lung and placenta may contribute to the lethality observed.

Impaired release of TGFα in the absence of TACE. The eye, hair, and skin defects associated with the *tace*$^{\Delta Zn}$ mutation are similar to those of mice lacking transforming growth factor-α (TGFα) (*15, 16*). TGFα is synthesized as a transmembrane precursor that is released from the cell surface by a metalloproteinase-dependent mechanism (*8*). To determine if the phenotypic similarities between *tace*$^{\Delta Zn/\Delta Zn}$ mice and TGFα-deficient mice could reflect a requirement for TACE in TGFα shedding, we compared the amounts of soluble and cell-associated TGFα in cultures of *tace*$^{\Delta Zn/\Delta Zn}$ and wild-type embryonic fibroblasts (immortalized by infection with a retrovirus encoding ras and myc). Release of soluble TGFα by *tace*$^{\Delta Zn/\Delta Zn}$ cells was reduced about 95% compared with that of wild-type cells (Fig. 2). Amounts of cell-associated TGFα in mutant and wild-type populations were comparable. Consistent with these data from cultured cells, highly purified recombinant TACE efficiently and correctly cleaved a peptide (*17*) representing the TGFα juxtamembrane processing site (Fig. 3A). These studies indicate a role for TACE in the proteolytic release of TGFα from the cell surface. Despite the biological activity of membrane-anchored TGFα defined in vitro (*18*), soluble TGFα is apparently essential for normal hair follicle development and eyelid fusion in vivo.

The additional epithelial defects observed in *tace*$^{\Delta Zn/\Delta Zn}$ fetuses are similar to those reported in mice lacking the epidermal growth factor

receptor (EGFR) (*19*), an obligate receptor for EGF, TGFα, amphiregulin, betacellulin, heparin-binding EGF, and epiregulin. These ligands are all synthesized as transmembrane precursors from which soluble ectodomains are released by metalloproteases (*8, 20*). Hence, TACE may also process one or more of these other ligands, and this processing may be essential for normal development.

Additional ectodomain shedding defects in cells lacking TACE. The observation that TACE is involved in the processing of two functionally and structurally unrelated proteins, TNF (a type II membrane protein) and TGFα (a type I membrane protein), suggested that it may have a broad role in ectodomain shedding. We therefore examined its role in the release of the adhesion molecule L-selectin and the p75 TNFR in *tace*$^{\Delta Zn/\Delta Zn}$ cell populations that expressed these proteins endogenously. Shedding of both of these proteins is metalloproteinase mediated, stimulated by activators of protein kinase C (PKC), and thought to have a role in the modulation of inflammatory responses (*21, 22*). Although unstimulated wild-type and *tace*$^{\Delta Zn/\Delta Zn}$ thymocytes expressed comparable amounts of surface L-selectin, stimulation of PKC by treating cells with phorbol 12-*N*-myristate 13-acetate (PMA) led to a reduction of surface expression only from wild-type cells (Fig. 4, A and B). The defect in L-selectin shedding by *tace*$^{\Delta Zn/\Delta Zn}$ thymocytes appeared not to result from an inability to respond to PMA, because expression of the activation antigen CD69 was normally upregulated by PMA in these cells (Fig. 4, C and D). Normal expression of the T lineage markers CD4 and CD8 by *tace*$^{\Delta Zn/\Delta Zn}$ thymocytes indicated that development of these cells was not grossly affected by the mutation (*12*). A peptide spanning the L-selectin processing site (*23*) was also correctly cleaved by purified TACE (Fig. 3B), further supporting a role for TACE in L-selectin shedding.

The release of p75 TNFR was examined on immortalized wild-type and *tace*$^{\Delta Zn/\Delta Zn}$ bone marrow–derived monocytic (DRM) cells. Wild-type and *tace*$^{\Delta Zn/\Delta Zn}$ DRM cells expressed similar amounts of surface p75 TNFR, but a PMA-induced decrease in the amount of p75 TNFR on the cell surface was only observed in wild-type DRM cells (Fig. 4, E and F). Additionally, wild-type DRM cells cultured for several hours in the presence of PMA, lipopolysaccharide, and interferon-γ released soluble p75 TNFR into the medium, whereas none was detected in the medium of *tace*$^{\Delta Zn/\Delta Zn}$ DRM cultures (*12*). Thus, TACE, initially identified as a TNF processing enzyme, also participates in the processing of TGFα, L-selectin, and p75 TNFR. In accord with such a role, TACE is expressed in all cell types examined (*3, 12*), many of which are not generally significant TNF-producing cells.

Mechanism of TACE action. The ectodomain-shedding defects in *tace*$^{\Delta Zn/\Delta Zn}$ cells and the phenotype of *tace*$^{\Delta Zn/\Delta Zn}$ mice provide genetic evidence of a role for TACE in the shedding of a structurally and functionally diverse group of membrane-anchored proteins. Two lines of evidence indicate that the multiple processing defects in *tace*$^{\Delta Zn/\Delta Zn}$ cells result directly from TACE deficiency. First, transfection of wild-type TACE into *tace*$^{\Delta Zn/\Delta Zn}$ fibroblasts increased shedding of cotransfected TNF and p75 TNFR (*24*), indicating that defective shedding of these proteins in *tace*$^{\Delta Zn/\Delta Zn}$ cells results from a defect in TACE and not in some linked gene whose function may have been affected by the targeted mutation. Second, although some ADAM family members may interact bio-

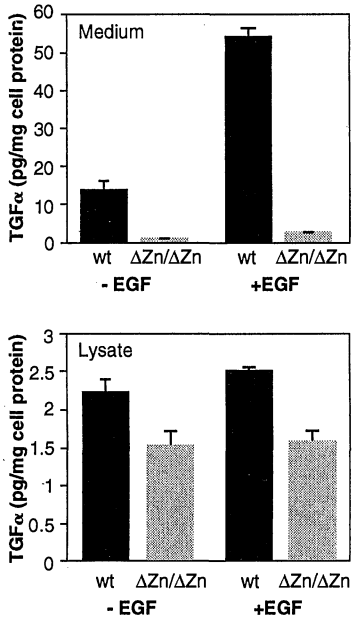

Fig. 2. TGFα shedding by wild-type and *tace*$^{\Delta Zn/\Delta Zn}$ fibroblasts. Wild-type (wt) and *tace*$^{\Delta Zn/\Delta Zn}$ (ΔZn/ΔZn) ras-myc–immortalized fibroblasts were cultured in the presence or absence of EGF, as indicated, for 24 hours and assayed for TGFα in the medium and cell lysate, as indicated, with a TGFα-specific radioimmunoassay (*32*). Inclusion of EGF in the medium increases the recovery of TGFα without interfering with the radioimmunoassay. Amounts of TGFα in the medium were normalized to protein concentration in the corresponding cell monolayer. Values represent the average of two replicates.

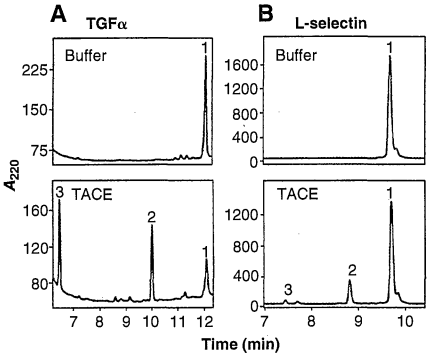

Fig. 3. Digestion of cleavage-site peptides. Peptides representing the cleavage sites in (**A**) TGFα (ADLLAVVAAS) (*33*) and (**B**) L-selectin (acetyl-KLDKSFSKIKEGDYN-amide) were incubated with buffer or TACE, as indicated, for 4 hours at 37°C and then analyzed by HPLC. Both peptides were based on human sequences, except that the methionine four residues downstream from the scissile bond in human L-selectin was replaced with lysine, which is found in this position in mouse L-selectin, to confer greater solubility to the peptide. In each case, peak 1 is the substrate. In (A), peak 2 is ADLLA and peak 3 is VVAAS. In (B), peak 2 is SFSKIKEGDYN-amide and peak 3 is acetyl-KLDK. The minor ultraviolet-absorbing species generated were not detected by the LC/MS procedure (*34*).

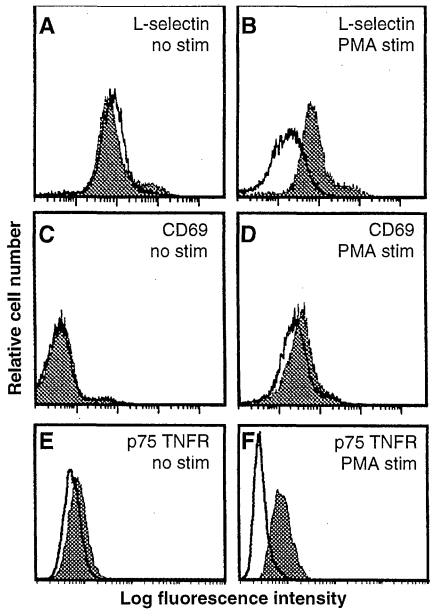

Fig. 4. L-Selectin and p75 TNFR shedding by wild-type and *tace*$^{\Delta Zn/\Delta Zn}$ cells. Flow cytometric analyses of thymocytes from a 2.5-week-old *tace*$^{\Delta Zn/\Delta Zn}$ mouse (shaded) and from a wild-type littermate (unshaded) stained for L-selectin (**A** and **B**) or CD69 (**C** and **D**), after no treatment [(A) and (C)] or stimulation with PMA (100 ng/ml) for 30 min [(B) and (D)]. Flow cytometric analyses of wild-type (unshaded) and *tace*$^{\Delta Zn/\Delta Zn}$ (shaded) DRM cells stained for p75 TNFR after no treatment (**E**) or stimulation with PMA (100 ng/ml) for 30 min (**F**). L-Selectin was detected with biotinylated antibody to muL-selectin (clone MEL-14, PharMingen) followed by streptavidin-conjugated phycoerythrin (PharMingen). CD69 was detected with fluorescein isothiocyanate–conjugated antibody to muCD69 (clone H1.2F3, PharMingen). p75 TNFR was detected with biotinylated antibody to murine p75 TNFR (clone TR75-54, Genzyme) in conjunction with streptavidin-conjugated phycoerythrin (PharMingen).

chemically (*25*) and overexpressed ADAMs lacking a catalytic domain can function as dominant negatives (*5*), it is unlikely that the *tace*$^{\Delta Zn}$ gene product, if expressed at the protein level (*26*), is functioning as a dominant negative with respect to other ADAM members because *tace*$^{\Delta Zn/+}$ mice have no phenotype, and shedding of various membrane proteins including TNF and L-selectin is normal in *tace*$^{\Delta Zn/+}$ cells (*12*).

These data suggest a critical role for TACE in the processing of multiple proteins. Although TACE could be an obligate component of a proteinase cascade, specific cleavage of processing-site peptides by TACE, and not by the structurally related metalloproteinase MMP-3 (*27, 28*), indicates that TACE may directly process multiple shed proteins. The strong interaction between TACE and a TNF peptide (cleavage was 9 times and 2250 times more efficient than with the TGFα and L-selectin peptides, respectively) could explain why TACE cleaves extracted TNF precursor protein whereas other apparent native substrates are not cleaved (*3, 28*). In these cases, membrane anchoring may be required to productively align the enzyme and its substrate (*22, 27, 29, 30*).

TACE may be a central component of the mechanism by which cells shed membrane proteins. Lethality in mice lacking TACE highlights the importance of TACE-directed ectodomain shedding during development. Although other metalloproteinases may also participate in the shedding of these apparent TACE substrates, therapeutic inhibitors of TNF release that target TACE may have activity against other shed proteins.

References and Notes

1. Disintegrin domains may encode integrin ligands that regulate intercellular and cell-matrix interactions.
2. C. P. Blobel *et al.*, *Nature* **356**, 248 (1992); T. G. Wolfsberg, P. Primakoff, D. G. Myles, J. M. White, *J. Cell. Biol.* **131**, 275 (1995).
3. R. A. Black *et al.*, *Nature* **385**, 729 (1997).
4. M. L. Moss *et al.*, *ibid.*, p. 733.
5. D. Pan and G. M. Rubin, *Cell* **90**, 271 (1997).
6. C. Wen, M. M. Metzstein, I. Greenwald, *Development* **124**, 4759 (1997).
7. N. M. Hooper, E. H. Karran, A. J. Turner, *Biochem. J.* **321**, 265 (1997).
8. J. Arribas *et al.*, *J. Biol. Chem.* **271**, 11376 (1996).
9. C. I. Brannan *et al.*, *Proc. Natl. Acad. Sci. U.S.A.* **88**, 4671 (1991); M. Grell *et al.*, *Cell* **83**, 793 (1995); T. Suda, H. Hashimoto, M. Tanaka, T. Ochi, S. Nagata, *J. Exp. Med.* **186**, 2045 (1997).
10. M. L. Heaney and D. W. Golde, *Blood* **87**, 847 (1996).
11. M. Pasparakis, L. Alexopoulou, V. Episkopou, G. Kollias, *J. Exp. Med.* **184**, 1397 (1996); M. W. Marino *et al.*, *Proc. Natl. Acad. Sci. U.S.A.* **94**, 8093 (1997); J. J. Peschon *et al.*, *J. Immunol.* **160**, 943 (1998).
12. J. J. Peschon and K. L. Stocking, data not shown.
13. M. J. Harris and M. J. McLeod, *Anat. Embryol.* **164**, 207 (1982).
14. J. J. Peschon and R. W. Boyce, data not shown.
15. N. C. Luetteke *et al.*, *Cell* **73**, 263 (1993).
16. G. B. Mann *et al.*, *ibid.*, p. 249; E. A. Berkowitz *et al.*, *Cell Growth Differ.* **7**, 1271 (1996).
17. J. Massagué, *J. Biol. Chem.* **265**, 21393 (1990).
18. S. T. Wong *et al.*, *Cell* **56**, 495 (1989); R. Brachmann *et al.*, *ibid.*, p. 691.
19. P. J. Miettinen *et al.*, *Nature* **376**, 337 (1995); M. Sibilia and E. F. Wagner, *Science* **269**, 234 (1995); D. W. Threadgill *et al.*, *ibid.*, p. 230.
20. D. C. Lee and K. M. Han, in *Peptide Growth Factors and Their Receptors*, vol. 95/II of *Handbook of Experimental Pharmacology*, M. B. Sporn and A. B. Roberts, Eds. (Springer-Verlag, Berlin, 1990), pp. 611–654; G. Raab *et al.*, *Biochem. Biophys. Res. Commun.* **204**, 592 (1994); M. Suzuki, G. Raab, M. A. Moses, C. A. Fernandez, M. Klagsbrun, *J. Biol. Chem.* **272**, 31730 (1997).
21. P. D. Crowe *et al.*, *J. Exp. Med.* **181**, 1205 (1995); T. A. Bennett, E. B. Lynam, L. A. Sklar, S. Rogelj, *J. Immunol.* **156**, 3093 (1996); C. Feehan *et al.*, *J. Biol. Chem.* **271**, 7019 (1996).
22. G. Preece, G. Murphy, A. Ager, *J. Biol. Chem.* **271**, 11634 (1996).
23. G. I. Migaki, J. Kahn, T. K. Kishimoto, *J. Exp. Med.* **182**, 549 (1995).
24. J. L. Slack, P. Reddy, R. A. Black, data not shown.
25. T. G. Wolfsberg *et al.*, *Proc. Natl. Acad. Sci. U.S.A.* **90**, 10783 (1993); C. P. Blobel, *Cell* **90**, 589 (1997).
26. Antibodies for reliably detecting endogenous murine TACE are unavailable.
27. K. Maskos *et al.*, *Proc. Natl. Acad. Sci. U.S.A.* **95**, 3408 (1998).
28. J. L. Slack and R. A. Black, data not shown.
29. S. S. Sisodia, *Proc. Natl. Acad. Sci. U.S.A.* **89**, 6075 (1992); H. J. Cheng and J. G. Flanagan, *Mol. Biol. Cell.* **5**, 943 (1994); S. B. Roberts, J. A. Ripellino, K. M. Ingalls, N. K. Robakis, K. M. Felsenstein, *J. Biol. Chem.* **269**, 3111 (1994); M. R. W. Ehlers *et al.*, *Biochemistry* **35**, 9549 (1996).
30. R. Sadhukhan, G. C. Sen, R. Ramchandran, I. Sen, *Proc. Natl. Acad. Sci. U.S.A.* **95**, 138 (1998).
31. Tissues were fixed in 10% neutral-buffered formalin, embedded in paraffin, sectioned, and stained with hematoxylin and eosin. Hair specimens were prepared as described, except that bovine serum was substituted for egg white (*15*).
32. E. P. Sandgren, N. C. Luetteke, R. D. Palmiter, R. L. Brinster, D. C. Lee, *Cell* **61**, 1121 (1990); W. E. Russell, P. J. Dempsey, S. Sitaric, A. J. Peck, R. J. Coffey Jr., *Endocrinology* **133**, 1731 (1993).
33. Single-letter abbreviations for the amino acid residues are as follows: A, Ala; C, Cys; D, Asp; E, Glu; F, Phe; G, Gly; H, His; I, Ile; K, Lys; L, Leu; M, Met; N, Asn; P, Pro; Q, Gln; R, Arg; S, Ser; T, Thr; V, Val; W, Trp; and Y, Tyr.
34. Peptides were either synthesized at Immunex (TNF, L-selectin) or obtained commercially (TGFα; SynPep). The enzyme used for the digests was a catalytic domain–polyHis construct expressed in Chinese hamster ovary cells and purified with Ni-nitrilotriacetic acid (Qiagen) and gel filtration columns (*27*). About 7 μM and 1.4 μM TACE was used for the L-selectin and TGFα peptides, respectively. All the incubations were with 0.5 mM peptide in 20 μl and were done for 0.5, 1, 2, and 4 hours at 37°C in 10 mM tris (pH 7.5). Digestion was a linear function of time in all cases, and the comparative data are based on the rates of the reactions. High-performance liquid chromatography (HPLC) analysis of products was done as described [R. A. Black *et al.*, *Biochem. Biophys. Res. Commun.* **225**, 400 (1996)]. The composition of the digests was determined by liquid chromatography/mass spectrometry (LC/MS), on a 1-mm ID Vydac C18 column with a flow rate of 50 μl/min and a linear gradient of 2% acetonitrile/min in 0.1% trifluoroacetate. LC/MS data were obtained by directing 10% of the HPLC effluent to the electrospray source of a Finnigan TSQ700 triple quadrupole mass spectrometer (San Jose, CA).

35. We thank the Immunex Animal Facility, the Flow Cytometry and Histology groups, K. Brasel, C. Willis, M. Glaccum, D. Barone, R. Blanton, K. Mohler, J. Schuh, and J. Doedens for their contributions to this work; H. Nagase of the University of Kansas Medical Center for providing MMP-3; M. Hall and G. Carlton for graphic assistance; and A. Aumell for help with manuscript preparation. Supported in part by NIH grants CA43793 (D.C.L.) and DK53804 (W.E.R.), and NSF grant MCB9729645 (W.E.R.).

25 June 1998; accepted 23 September 1998

Presolar Corundum and Spinel in Ordinary Chondrites: Origins from AGB Stars and a Supernova

Byeon-Gak Choi,* Gary R. Huss, G. J. Wasserburg, Roberto Gallino

On the basis of anomalous isotopic compositions of oxygen and magnesium, 14 oxide grains from two primitive meteorites (Bishunpur and Semarkona) have been identified as circumstellar condensates. One corundum grain has a high $^{18}O/^{16}O$ ratio and isotopic compositions of magnesium, calcium, and titanium that are compatible with a formation in ejecta of a type II supernova that was about 15 times the mass of the sun. The other grains have oxygen, magnesium, and titanium compositions that are consistent with a formation around asymptotic giant branch (AGB) stars with a range of mass and initial composition. The large range of aluminum/magnesium in circumstellar corundum and spinel is considered to reflect various stages of back-reaction between condensed corundum and gaseous magnesium in cooling stellar ejecta.

Presolar grains that were extracted from primitive meteorites existed before the formation of the solar system. Most grains are circumstellar condensates that formed in stellar ejecta. They provide a unique opportunity to study nucleosynthesis in stars and to study condensation processes in the wind of mass-losing AGB stars and in supernova ejecta. The most abundant circumstellar condensates recovered are carbon-rich phases [diamond, graphite, silicon carbide, and titanium carbide (*1, 2*)]. Presolar oxides, which should have been abundant in the solar nebula, have been difficult to identify because of the over-